Inorganic Chemistry
Article

Inorg. Chem. **2009**, *48*, 9567–9578 **9567**
DOI: 10.1021/ic901407d

Design and Synthesis of a Stable Supramolecular Trigonal Prism Formed by the Self-Assembly of a Linear Tetrakis(Zn^{2+}−cyclen) Complex and Trianionic Trithiocyanuric Acid in Aqueous Solution and Its Complexation with DNA (Cyclen = 1,4,7,10-Tetraazacyclododecane)

Mohd Zulkefeli,[†,‡] Tetsuya Sogon,[§] Kei Takeda,[§] Eiichi Kimura,[§] and Shin Aoki*[,†,∥]

[†]*Faculty of Pharmaceutical Sciences, Tokyo University of Science, 2641 Yamazaki, Noda, Chiba, 278-8510 Japan,* [‡]*Faculty of Pharmacy, Universiti Teknologi MARA, Puncak Alam, Selangor, 42300, Malaysia,* [§]*Division of Medicinal Chemistry, Graduate School of Biomedical Sciences, Hiroshima University, 1-2-3 Kasumi, Minami-ku, Hiroshima, 734-8551 Japan, and* [∥]*Center for Technologies against Cancer, Tokyo University of Science, 2641 Yamazaki, Noda, Chiba, 278-8510 Japan*

Received July 18, 2009

A new supramolecular complex, $\{(Zn_4L^4)_3-(TCA^{3-})_4\}^{12+}$, was designed and synthesized by the 3:4 self-assembly of a linear tetrakis(Zn^{2+}−cyclen) complex $(Zn_4L^4)^{8+}$ and trianionic trithiocyanurate (TCA^{3-}) in aqueous solution (cyclen = 1,4,7,10-tetraazacyclododecane). The $\{(Zn_4L^4)_3-(TCA^{3-})_4\}^{12+}$ complex, which should have a trigonal prism configuration, was found to be very stable in aqueous solution at neutral pH and 25 °C, as evidenced by ^{1}H NMR titration, potentiometric pH and UV titrations, and MS measurements. The complex does not dissociate into the starting building blocks in the presence of Zn^{2+}-binding anions such as phosphates and double-stranded DNA. The results of the competitive binding assays with ethidium bromide and calf-thymus DNA, thermal melting experiments, gel mobility shift assays, and dynamic light-scattering data strongly indicated that the trigonal prism functions as a polycationic template to induce the aggregation of double-stranded DNA.

Introduction

Multicomponent self-assembly by means of metal−ligand coordination is a subject of considerable interest in the area of supramolecular chemistry.[1] Supramolecular chemistry in aprotic solvents is currently a well-developed area of study.[2] For example, Lehn and co-workers have reported on the formation of grid-type three-dimensional architectures using the self-assembly of pyridine-based and pyrimidine-based ligands with Cu^{1+}, Ag^{1+}, Mn^{2+}, Pb^{2+}, Co^{2+}, Zn^{2+}, and Fe^{2+}.[3] It should be noted, however, that molecular recognition and discrimination in nature takes place largely in aqueous media. Because strong hydration disturbs nonconvalent molecular interactions in aqueous solution, the design and synthesis of supramolecular complexes that interact with biological macromolecules in aqueous solution represents a challenging task.[4]

A wide variety of water-soluble supramolecular complexes, prepared using different molecular structures, have been reported to date. For example, Fujita and co-workers

*To whom correspondence should be addressed. E-mail: shinaoki@rs.noda.tus.ac.jp.

(1) (a) Coon, M. M.; Rebek, J., Jr. *Chem. Rev.* **1997**, *97*, 1647–1668. (b) Caulder, D. L.; Raymond, K. N. *J. Chem. Soc., Dalton Trans.* **1999**, 1185–1200. (c) Ward, M. D.; McCleverty, J. A.; Jeffery, J. C. *Coord. Chem. Rev.* **2001**, *222*, 251–272. (d) Sun, W.-Y.; Yoshizawa, M.; Kasukawa, T.; Fujita, M. *Curr. Opin. Chem. Biol.* **2002**, *6*, 757–764. (e) Park, K.-M.; Whang, D.; Lee, E.; Heo, J.; Kim, K. *Chem.—Eur. J.* **2002**, *8*, 498–508. (f) Fujita, M; Tominaga, M; Hori, A.; Therrien, B. *Acc. Chem. Res.* **2005**, *38*, 371–380. (g) Friedler, D.; Leung, D. H.; Bergman, R. G.; Raymond, K. N. *Acc. Chem. Res.* **2005**, *38*, 349–358. (h) Lützen, A. *Angew. Chem., Int. Ed.* **2005**, *44*, 1000–1002. (i) Pluth, M; Raymond, K. N. *Chem. Soc. Rev.* **2007**, *36*, 161–171. (j) Kumar, A.; Sun, S.-S.; Lees, A. J. *Coord. Chem. Rev.* **2008**, *252*, 922–939.

(2) (a) Amabilino, D. B.; Ashton, P. R.; Balzani, V.; Brown, C. L.; Credi, A.; Frchet, J. M. L.; Leon, J. W.; Raymo, F. M.; Spencer, N.; Stoddart, J. F.; Venturi, M. *J. Am. Chem. Soc.* **1996**, *118*, 12012–12020. (b) Ryan, D.; Rao, S. N.; Rensmo, H.; Fitmaurice, D.; Preece, J. A.; Wenger, S.; Stoddart, J. F.; Zaccheroni, N. *J. Am. Chem. Soc.* **2000**, *122*, 6252–6257. (c) Raymo, F. M.; Bartberger, M. D.; Honk, K. N.; Stoddart, J. F. *J. Am. Chem. Soc.* **2001**, *123*, 9264–9267. (d) Hernandez, R.; Tseng, H.-R.; Wong, J. W.; Stoddart, J. F.; Zink, J. I. *J. Am. Chem. Soc.* **2004**, *126*, 3370–3371. (e) Park, J.; Lang, K.; Abboud, K. A.; Houg, S. *J. Am. Chem. Soc.* **2008**, *130*, 16484–16485.

(3) (a) Balaban, T. S.; Goddard, R.; Linke-Schaetzel, M.; Lehn, J.-M. *J. Am. Chem. Soc.* **2003**, *125*, 4233–4239. (b) Barboiu, M.; Vaughan, G.; Graff, R.; Lehn, J.-M. *J. Am. Chem. Soc.* **2003**, *125*, 10257–10265. (c) Ruben, M.; Rojo, J.; Romeo-Salguero, F. J.; Uppadine, L. H.; Lehn, J.-M. *Angew. Chem., Int. Ed.* **2004**, *43*, 3644–3662. (d) Ramirez, J.; Stadler, A.-M.; Rogez, G.; Drillon, M.; Lehn, J.-M. *Inorg. Chem.* **2009**, *48*, 2456–2463.

(4) (a) Prins, L. J.; Reinhoudt, D. N.; Timmerman, P. *Angew. Chem., Int. Ed.* **2001**, *40*, 2382–2426. (b) Atwood, J. L.; Leonard, J. B.; Agoston, J. *Science* **2002**, *296*, 2367–2369. (c) Kubik, S.; Reheller, C.; Stüwe, S. *J. Incl. Phenom. Macrocycl. Chem.* **2005**, *52*, 137–187. (d) Schmuck, C. *Angew. Chem., Int. Ed.* **2007**, *46*, 5830–5833. (e) Oshovsky, G. V.; Reinhoudt, D. N.; Verboom, W. *Angew. Chem., Int. Ed.* **2007**, *46*, 2366–2393.

Published on Web 09/10/2009

reported on the formation of cagelike supramolecular complexes in aqueous solution on the basis of the concept of molecular paneling using coordination bonds between polypyridyl ligands and Pd^{2+} or Pt^{2+} complexes.[5] Raymond and co-workers reported on supramolecular host systems by using Ga^{3+}, Al^{3+}, Ti^{4+}, Ge^{4+}, and Fe^{3+} as template metal cations.[6] In general, those supramolecules possess a hydrophobic inner cavity and serve as molecular recognition site and reaction vessels for organic guest molecules. Despite these reports on supramolecular assembling, most systems for small guest molecules comprised of supramolecular systems that interact with biological macromolecules in aqueous media have been limited.[7,8]

The zinc ion (Zn^{2+}) is a transition metal that is ubiquitous in natural biological systems. To date, more than 300 molecular structures that involve the functionality of Zn^{2+} proteins and Zn^{2+} enzymes have been reported.[9] The Zn^{2+} sites of Zn^{2+}-containing proteins can be classified into three categories: a structural factor in zinc finger proteins and zinc(II) enzymes, such as alcohol dehydrogenase; a catalytic factor, as in zinc(II) enzymes including carbonic anhydrase and alcohol dehydrogenase; and a cocatalytic factor, as found in some aminopeptidases.[10]

It has been established that Zn^{2+} complexes of macrocyclic polyamines such as $Zn^{2+}-$cyclen **1** $(ZnL^1)^{2+}$ are stable in aqueous solution at neutral pH (Scheme 1) and are good models for Zn^{2+} enzymes such as carbonic anhydrase, alkaline phosphatase, and related enzymes (cyclen = 1,4,7,10-tetraazacyclododecane).[11] These Zn^{2+} complexes form 1:1 complexes ($\mathbf{1}-X^-$ complex) with various anions including carboxylates,[12] phosphates,[13] imides (such as thymine),[14] and thiolates.[15,16]

Our current interest is in molecular assembly systems that involve the formation of multiple coordination bonds between multinuclear Zn^{2+} complexes and polyanionic compounds.[17,18] We previously reported that the self-assembly of

(5) (a) Fujita, M. *Molecular Self-Assembly Organic Versus Inorganic Approaches*; Springer: Berlin, 2000; Vol. *96*. (b) Fujita, M.; Umemoto, K.; Yoshizawa, M.; Fujita, N.; Kusukawa, T.; Biradha, K. *J. Chem. Soc., Chem. Commun*. **2001**, 509–518. (c) Kusukawa, T.; Fujita, M. *J. Am. Chem. Soc*. **2002**, *124*, 13576–13582. (d) Nakabayashi, K.; Kawano, M.; Yoshizawa, M.; Ohkoshi, S.-I.; Fujita, M. *J. Am. Chem. Soc*. **2004**, *126*, 16694–16695. (e) Yoshizawa, M.; Fujita, M. *Pure. Appl. Chem*. **2005**, *77*, 1107–1112. (f) Fujita, M.; Tominaga, M.; Hori, A.; Therrien, B. *Acc. Chem. Res*. **2005**, *38*, 371–380. (g) Kawano, M.; Kobayashi, Y.; Ozeki, T.; Fujita, M. *J. Am. Chem. Soc*. **2006**, *128*, 6558–6559. (h) Maurizot, V.; Yoshizawa, M.; Kawano, M.; Fujita, M. *Dalton Trans*. **2006**, 2750–2756. (i) Suzuki, K.; Kawano, M.; Sato, S.; Fujita, M. *J. Am. Chem. Soc*. **2007**, *129*, 10652–10653. (j) Yamauchi, Y.; Yoshizawa, M.; Fujita, M. *J. Am. Chem. Soc*. **2008**, *130*, 5832–5833.

(6) (a) Caulder, D. L.; Raymond, K. N. *Acc. Chem. Res*. **1999**, *32*, 975–982. (b) Brumaghim, J. L.; Martin, M.; Raymond, K. N. *Eur. J. Org. Chem*. **2004**, *24*, 4552–4559. (c) Seeber, G.; Tiedemann, B. E. F.; Raymond, K. N. *Top. Curr. Chem*. **2006**, *265*, 147–183. (d) Fiedler, D.; Halbeek, H. V.; Bergman, R. G.; Raymond, K. N. *J. Am. Chem. Soc*. **2006**, *128*, 10240–10252. (e) Biros, S. M.; Bergman, R. G.; Raymond, K. N. *J. Am. Chem. Soc*. **2007**, *129*, 12094–12095.

(7) (a) Linton, B.; Hamilton, A. D. *Chem. Rev*. **1997**, *97*, 1669–1680. (b) Babine, R. E.; Bender, S. L. *Chem. Rev*. **1997**, *97*, 1359–1472. (c) Davis, J. M.; Tsou, L. K.; Hamilton, A. D. *Chem. Soc. Rev*. **2007**, *36*, 326–334. (d) Sawada, T.; Yoshizawa, M.; Sato, S.; Fujita, M. *Nature Chem*. **2009**, *1*, 53–56.

(8) (a) Meistermann, I.; Moreno, V.; Prieto, M. J.; Moldrheim, E.; Sletten, E.; Khalid, S.; Rodger, P. M.; Peberdy, J. C.; Isaac, C. J.; Rodger, A.; Hannon, M. J. *Proc. Natl. Acad. Sci. U. S. A*. **2002**, *99*, 5069–5074. (b) Oleksi, A.; Blanco, A. G.; Boer, R.; Uso′n, I.; Aymami, J.; Rodger, A.; Hannon, M. J.; Coll, M. *Angew. Chem., Int. Ed*. **2006**, *45*, 1227–1231. (c) Cerasimo, L.; Hannon, M. J.; Sletten, E. *Inorg. Chem*. **2007**, *46*, 6245–6251. (d) Hannon, M. J. *Chem. Soc. Rev*. **2007**, *36*, 280–295.

(9) (a) Vallee, B. L.; Auld, D. S. *Proc. Natl. Acad. Sci. U. S. A*. **1990**, *87*, 220–224. (b) Christianson, D. W. *Adv. Prot. Chem*. **1991**, *42*, 281–335. (c) Coleman, J. E. *Annu. Rev. Biochem*. **1992**, *61*, 897–946.

(10) (a) Cotton, F. A.; Wilkinson, G. *Advanced Inorganic Chemistry: A Comprehensive Text*, 5th ed., Vol *1*; John Wiley & Sons: New York, 1988. (b) Arnold, F. H.; Haymore, B. L. *Science* **1991**, *252*, 1796–1797. (c) Vallee, B. L.; Falchuk, K. H. *Phys. Rev*. **1993**, *73*, 79–118. (d) Vallee, B. L.; Auld, D. S *Acc. Chem. Rev* **1993**, *26*, 543–551. (e) Christianson, D. W.; Cox, J. D. *Annu. Rev. Biochem*. **1999**, *68*, 33–57. (f) Auld, D. S. *Biometals* **2001**, *14*, 271–313.

(11) (a) Kimura, E.; Koike, T. In *Comprehensive Supramolecular Chemistry*; Reinhoudt, D. N., Ed.; Pergamon: Tokyo, 1996; Vol. *10*, pp 429−444. (b) Koike, T.; Watanabe, T.; Aoki, S.; Kimura, E.; Shiro, M. *J. Am. Chem. Soc*. **1996**, *118*, 12696–12703. (c) Kimura, E. *S. Afr. J. Chem*. **1997**, *50*, 240–248. (d) Kimura, E.; Koike, T.; Shionoya, M. In *Structure and Bonding: Metal Site in Proteins and Models*; Sadler, J. P., Ed.; Springer: Berlin, 1997; Vol. *89*, pp 1−28. (e) Kimura, E.; Koike, T. *Chem. Soc. Rev*. **1998**, *27*, 179–184. (f) Kimura, E.; Koike, T. In *Bioinorganic Catalysis*; Reedijk, J., Bouwman, E., Eds.; Marcel Dekkar, Inc: New York, 1999; pp 33−54. (g) Kimura, E.; Kikuta, E. *J. Biol. Inorg. Chem*. **2000**, *5*, 139–155. (h) Kimura, E. *Curr. Opin. Chem. Biol*. **2000**, *4*, 207–213. (i) Kimura, E. *Acc. Chem. Res*. **2001**, *34*, 171–179. (j) Kimura, E.; Aoki, S. *BioMetals* **2001**, *14*, 191–204. (k) Aoki, S.; Kimura, E. *Rev. Mol. Biotech*. **2002**, *90*, 129–155. (l) Aoki, S.; Kimura, E. *Chem. Rev*. **2004**, *104*, 769–787. (m) Kimura, E.; Takasawa, R.; Tanuma, S.; Aoki, S. *Science STKE* **2004**, 17.

(12) Kimura, E.; Ikeda, T.; Shionoya, M.; Shiro, M. *Angew. Chem., Int. Ed. Engl*. **1995**, *34*, 663–664.

(13) (a) Kimura, E.; Shiota, T.; Koike, T.; Shiro, M.; Kodama, M. *J. Am. Chem. Soc*. **1990**, *112*, 5805–5811. (b) Koike, T.; Kimura, E.; Nakamura, I.; Hashimoto, Y.; Shiro, M. *J. Am. Chem. Soc*. **1992**, *114*, 7338–7345. (c) Zhang, X.; van Eldik, R.; Koike, T.; Kimura, E. *Inorg. Chem*. **1993**, *32*, 5749–5755. (d) Fujioka, H.; Koike, T.; Yamada, N.; Kimura, E. *Heterocycles* **1996**, *42*, 775–787. (e) Kimura, E.; Aoki, S.; Koike, T.; Shiro, M. *J. Am. Chem. Soc*. **1997**, *119*, 3068–3076. (f) Aoki, S.; Kimura, E. *J. Am. Chem. Soc*. **2000**, *122*, 4542–4548. (g) Aoki, S.; Iwaida, K.; Hanamoto, N.; Shiro, M.; Kimura, E. *J. Am. Chem. Soc*. **2002**, *124*, 5256–5257.

(14) (a) Shionoya, M.; Kimura, E.; Shiro, M. *J. Am. Chem. Soc*. **1993**, *115*, 6730–6737. (b) Shionoya, M.; Ikeda, T.; Kimura, E.; Shiro, M. *J. Am. Chem. Soc*. **1994**, *116*, 3848–3859. (c) Koike, T.; Takashige, M.; Kimura, E.; Fujioka, H.; Shiro, M. *Chem.—Eur. J*. **1996**, *2*, 617–623. (d) Kimura, E.; Ikeda, T.; Aoki, S.; Shionoya, M. *J. Biol. Inorg. Chem*. **1998**, *3*, 259–267. (e) Aoki, S.; Honda, Y.; Kimura, E. *J. Am. Chem. Soc*. **1998**, *120*, 10018–10026. (f) Aoki, S.; Sugimura, C.; Kimura, E. *J. Am. Chem. Soc*. **1998**, *120*, 10094–10102. (g) Kikuta, E.; Murata, M.; Katsube, N.; Koike, T.; Kimura, E. *J. Am. Chem. Soc*. **1999**, *121*, 5426–5436. (h) Kimura, E.; Kikuta, E. *Prog. React. Kinet. Mech*. **2000**, *25*, 1–64. (i) Kimura, E.; Kitamura, H.; Ohtani, K.; Koike, T. *J. Am. Chem. Soc*. **2000**, *122*, 4668–4677. (j) Kikuta, E.; Aoki, S.; Kimura, E. *J. Am. Chem. Soc*. **2001**, *123*, 7911–7912. (k) Kikuta, E.; Aoki, S.; Kimura, E. *J. Biol. Inorg. Chem*. **2002**, *7*, 473–482. (l) Kimura, E.; Katsube, N.; Koike, T.; Shiro, M.; Aoki, S. *Supramol. Chem*. **2002**, *14*, 95–102. (m) Gasser, G.; Belousoff, M. J.; Bond, A. M.; Kosowski, Z.; Spiccia, L. *Inorg. Chem*. **2007**, *46*, 1665–1674.

(15) Aoki, S.; Kagata, D.; Shiro, M.; Takeda, K.; Kimura, E. *J. Am. Chem. Soc*. **2004**, *126*, 13377–13390.

(16) For reviews of anion receptors and sensors, see: (a) Lehn, J.-M. *Supramolecular Chemistry: Concepts and Perspectives*; VCH: Weinheim, Germany, 1995. (b) *Supramolecular Chemistry of Anions*; Bianchi, A., Bowman-James, K., Garcia-Espana, E., Eds.; Wiley-VCH: New York, 1996. (c) Sessler, J. L.; Andrievsky, A.; Genge, J. W. In *Advances in Supramolecular Chemistry*; Gokel, G. W., Ed.; JAI Press Inc.: Greenwich, CT, 1997; Vol. *4*, pp 97−142. (d) de Silva, A. P.; Nimal Gunaratne, H. Q.; Gunnlaugsson, T.; Huxley, A. J. M.; McCoy, C. P.; Rademacher, J. T.; Rice, T. E. *Chem. Rev*. **1997**, *97*, 1515–1566. (e) Schmidtchen, F. P.; Berger, M. *Chem. Rev*. **1997**, *97*, 1609–1646. (f) Beer, P. D. *Acc. Chem. Res*. **1998**, *31*, 71–80. (g) Beer, P. D.; Cadman, J. *Coord. Chem. Rev*. **2000**, *205*, 131–155. (h) Anzenbacher, P., Jr; Try, A. C.; Miyaji, H.; Jursazíková, K.; Lynch, V. M.; Marquez, M.; Sessler, J. L. *J. Am. Chem. Soc*. **2000**, *122*, 10268–10272. (i) Amendola, V.; Basteianello, E.; Fabbrizzi, L.; Mangano, C.; Pallavicini, P.; Perotti, A.; Lanfredi, A. M.; Ugozzoli, F. *Angew. Chem., Int. Ed*. **2000**, *39*, 2917–2920. (j) Peczuh, M. W.; Hamilton, A. D. *Chem. Rev*. **2000**, *100*, 2479–2494. (k) Beer, P. D.; Gale, P. A. *Angew. Chem., Int. Ed*. **2001**, *40*, 487–516. (l) Wiskur, S. L.; Ait-Haddou, H.; Anslyn, E. V.; Lavigne, J. J. *Acc. Chem. Res*. **2001**, *34*, 963–972. (m) Choi, K.; Hamilton, A. D. *J. Am. Chem. Soc*. **2001**, *123*, 2456–2457. (n) Rekharsky, M.; Inoue, Y.; Tobey, S.; Metzger, A.; Anslyn, E. *J. Am. Chem. Soc*. **2002**, *124*, 14959–14967. (o) Tobey, S. L.; Anslyn, E. V. *J. Am. Chem. Soc*. **2003**, *125*, 14807–14815. (p) Sakamoto, T.; Ojida, A.; Hamachi, I. *Chem. Commun*. **2009**, *125*, 141–152. (q) Wada, A.; Tamaru, S.; Ikeda, M.; Hamachi, I. *J. Am. Chem. Soc*. **2009**, *131*, 5321–5330.

(17) (a) Aoki, S.; Shiro, M.; Koike, T.; Kimura, E. *J. Am. Chem. Soc*. **2000**, *122*, 576–584. (b) Aoki, S.; Shiro, M.; Kimura, E. *Chem.—Eur. J*. **2002**, *8*, 929–939.

(18) Aoki, S.; Zulkefeli, M.; Shiro, M.; Kimura, E. *Proc. Natl. Acad. Sci. U. S. A*. **2002**, *99*, 4894–4899.

Scheme 1

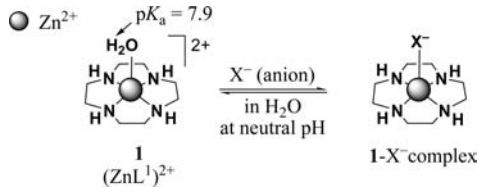

bis(Zn^{2+}−cyclen) **2** $(p\text{-}Zn_2L^2)^{4+}$ and linear tris(Zn^{2+}−cyclen) **4** $(p,p\text{-}Zn_3L^3)^{6+}$ with trianionic trithiocyanurate (TCA^{3-}) affords the 3:2 complex **3**, $\{(p\text{-}Zn_2L^2)_3{-}(TCA^{3-})_2\}^{6+}$, and the 3:3 complex **5**, $\{(p,p\text{-}Zn_3L^3)_3{-}(TCA^{3-})_3\}^{9+}$, respectively (Scheme 2).[18,19] In **3** and **5**, the deprotonated TCA (the pK_a values of TCA are 5.1 (pK_{a1}), 8.2 (pK_{a2}), and 11.7 (pK_{a3})) binds to **2** or **4** as a tridentate donor through Zn^{2+}−S(TCA^{3-}) and Zn^{2+}−N(TCA^{3-}) coordination bonds. The outer structures of **3** and **5** can be represented as trigonal prisms, as shown in Scheme 2.

In this manuscript, we describe the preparation of the supramolecular trigonal prism **7**, formed by the 3:4 assembly of the linear tetrakis(Zn^{2+}−cyclen) complex **6** $(Zn_4L^4)^{8+}$ and TCA^{3-} (Scheme 3). ^{1}H NMR, UV, and potentiometric pH titrations confirm that **7** is much more stable than the previously prepared trigonal prisms **3** and **5**. It is also noteworthy that **7** forms a complex with double-stranded DNA and inhibits the interaction of DNA with ethidium bromide (EB; a DNA intercalator) and 4′,6-diamidino-2-phenylindole (DAPI) and pentamidine (4,4′-[pentane-1,5-diylbis(oxy)]dibenzenecarboximidamide) (DNA minor groove binders). The results of gel mobility shift assays (GMSA) and dynamic light-scattering (DLS) of the **7**−DNA complex are also presented below.

Results and Discussion

Synthesis of 6 (Zn_4L^4). Linear tetrakis(cyclen) **13**, (L^4), and its Zn^{2+} complex **6**, $(Zn_4L^4)^{8+}$, were synthesized as shown in Scheme 4. The reaction of 3Boc-cyclen **8**[13e] with *p*-bis(bromomethylbenzene) gave **9**,[20] which was reacted with **10**, in which 1,7-nitrogen atoms in the cyclen ring were protected with diethylphosphate groups,[21] to give **11** in 51% yield. Dimerization of **11** with *p*-bis(bromomethylbenzene) yielded the fully protected tetrakiscyclen **12** (6Boc·4Dep−L^4), followed by deprotection of the Boc and Dep groups by treatment with aqueous HBr to give **13** as a 12HBr salt ($L^4\cdot 12HBr\cdot 2H_2O$). Neutralization of the **13**·HBr salt gave acid-free (L^4), which was complexed with four Zn^{2+} ions to give **6**.

Deprotonation Constants for Zn^{2+}-Bound Waters of 6 (Zn_4L^4) Determined by Potentiometric pH Titration. Potentiometric pH titrations of **6**, $(Zn_4L^4)^{8+}$ (0.6 mM), were carried out against 0.1 M NaOH with $I = 0.1$ at 25 °C. The pH titration curve for **6** (curve a in Figure 1) was analyzed for acid−base equilibrium, as defined by eq 1 (a_{H+} is the activity of H^+) using the "BEST" software program.[22] The deprotonation constants, pK_{ai} ($i = 1-4$), of the four Zn^{2+}-bound waters of **6** were determined to be 6.9 ± 0.1, 7.1 ± 0.1, 8.3 ± 0.1, and 8.5 ± 0.1, as listed in Table 1, with the pK_{ai} values of previous Zn^{2+} complexes, **1**, $(ZnL^1)^{2+}$; **2**, $(p\text{-}Zn_2L^2)^{4+}$; and **4**, $(p,p\text{-}Zn_3L^3)^{6+}$, indicating that the deprotonation of these four Zn^{2+}-bound waters occurs independently, as observed for **2** and **4**.[13e,18,20]

$$Zn_4L^4\cdot(H_2O)_{(5-i)}\cdot(HO^-)_{(i-1)} \rightleftarrows Zn_4L^4\cdot(H_2O)_{(4-i)}\cdot(HO^-)_i + H^+ \quad (i = 1-4)$$

$$K_{ai} = [Zn_4L^4\cdot(H_2O)_{(4-i)}\cdot(HO^-)_i]a_{H^+}/[Zn_4L^4\cdot(H_2O)_{(5-i)}\cdot(HO^-)_{(i-1)}] \quad (1)$$

Complexation of 6, $(Zn_4L^4)^{8+}$, with TCA^{3-} in Aqueous Solution Determined by ^{1}H NMR Titration. Figure 2 shows the results of ^{1}H NMR titrations of **6** with TCA in D_2O at a pD of 8.0 ± 0.1 and at 25 °C. In Figure 2a, ^{1}H NMR signals of aromatic protons of uncomplexed **6** (3.0 mM) were observed at ca. 7.5 ppm. Upon the addition of 2.0 mM TCA (0.66 equiv against **6**), one set of new ^{1}H peaks appeared at δ 7.17, 7.04, and 6.94 ppm, as indicated by the plain arrows in Figure 2b. In the presence of 4.0 mM (1.33 equiv against **6**) and 6.0 mM (2.0 equiv against **6**) TCA, the ^{1}H signals of free **6** disappeared (Figure 2c and d), indicating that the 3:4 complexation of **7** and TCA occurred, as predicted. The fact that two independent ^{1}H signals were observed upon complexation with TCA indicates that the complex formed from **6** and TCA^{3-} is not only thermodynamically but kinetically stable on the NMR time scale. The addition of 10−20 equiv of Cl^-, Br^-, and SO_4^{2-} resulted in negligible changes of the ^{1}H NMR spectra (data not shown). The broad singlet at δ 7.2 and two distinct doublets (at δ 7.04 and 6.94) are found in Figure 2c, although the aromatic protons of uncomplexed **6** were observed as broad, singletlike signals at ca. δ 7.5 ppm (Figure 2a). The same phenomena were observed in ^{1}H NMR spectra of the trigonal prism **5** formed by the 3:3 assembly of **4** and TCA.[18]

Our previous results of an X-ray crystal structure analysis of **5** revealed that the central TCA in **5** is coordinated to Zn^{2+} through Zn^{2+}−N and Zn^{2+}−S coordination bonds, while the two TCA molecules at the terminus in **5** bind to Zn^{2+} ions through Zn^{2+}−S coordination bonds, as displayed in Scheme 5. These different coordination modes of TCA^{3-} units resulted in a different environment of the benzene protons of **5** near the middle TCA and terminal TCA, as observed in ^{1}H NMR spectra. Analogously, we assume that two terminal TCA^{3-} ions in **7** coordinate to Zn^{2+} through Zn^{2+}−S coordination bonds and the two central TCA^{3-} ions bind to Zn^{2+} through Zn^{2+}−N and Zn^{2+}−S coordination bonds, as depicted in Scheme 5 (lower part).

UV Spectrophotometric Titrations of 6, $(Zn_4L^4)^{8+}$. We conducted UV spectrophotometric titrations of TCA (30 μM) with **6** in 10 mM HEPES (pH 7.4) with $I = 0.1$ ($NaNO_3$) at 25 °C. As shown in Figure 3, the uncomplexed TCA shows an absorption maximum (λ_{max}) at 283 nm ($\varepsilon = 4.1 \times 10^4$ (M^{-1} cm^{-1})) and 323 nm ($\varepsilon = 2.8 \times 10^4$ (M^{-1} cm^{-1})) at pH 7.4 (where [TCA]/[TCA^-]/[TCA^{2-}]/[TCA^{3-}] distribution is

(19) As suggested by the reviewer, we mention the positive charges of the supramolecular complexes by using the fences "{ }" in this manuscript, because brackets "[ ]" are normally used to represent the concentrations of compounds including their cationic or anionic species.

(20) Kimura, E.; Kikuchi, M.; Kitamura, H.; Koike, T. *Chem.—Eur. J.* **1999**, *5*, 3113–3123.

(21) Dumont, A.; Jacques, V.; Desreux, J. F. *Tetrahedron Lett.* **1994**, *35*, 3707–3710.

(22) Martell, A. E.; Motekaitis, R. J. *Determination and Use of Stability Constants*, 2nd ed.; VCH: New York, 1992.

Scheme 2

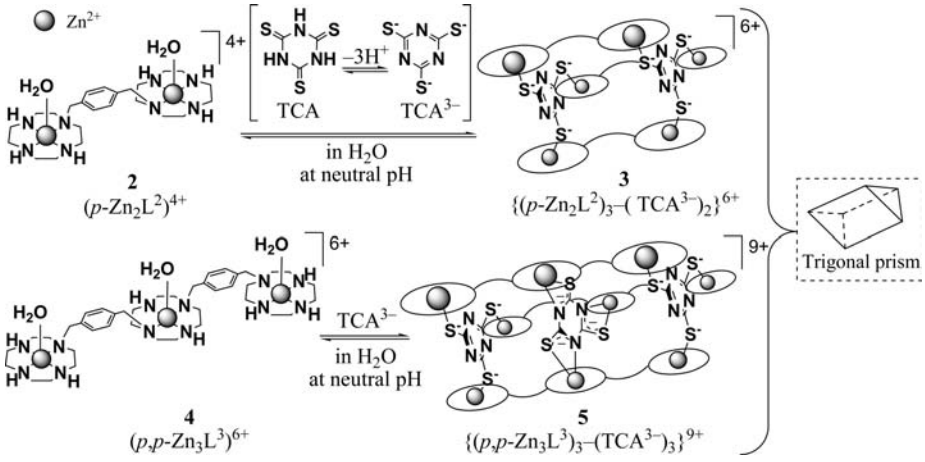

Scheme 3

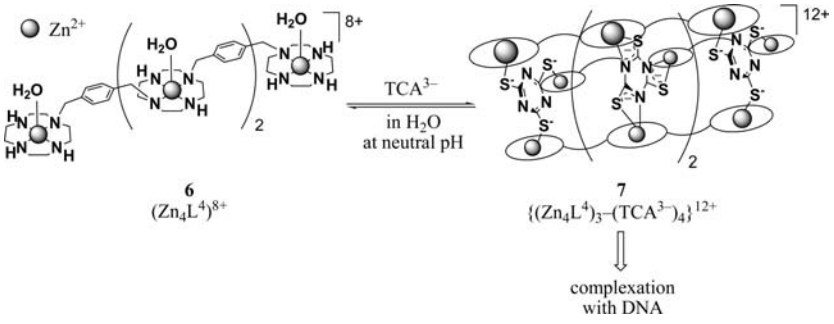

Scheme 4

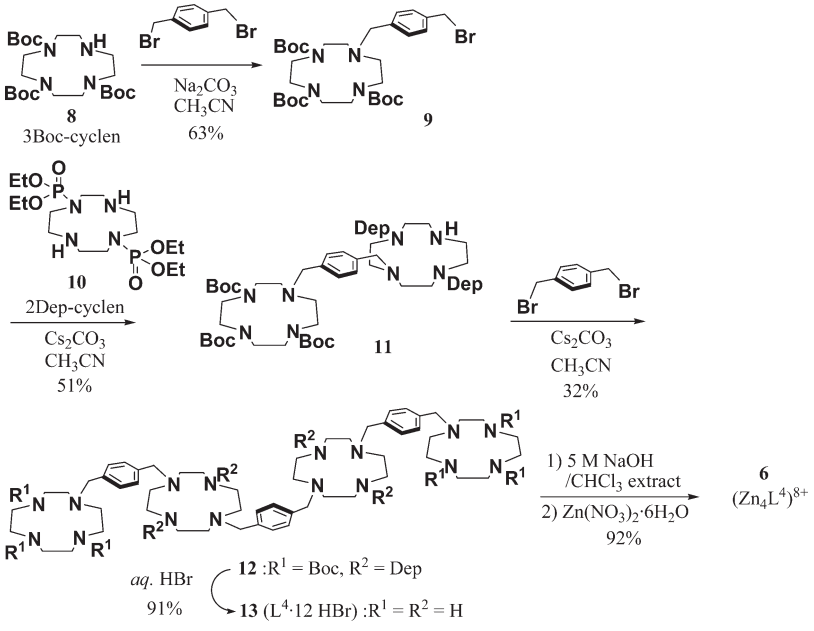

estimated to be 1:96:6:0 from the three pK_a values of TCA). The addition of complex **6** induced a decrease in this absorption, analogous to that for the UV titration of TCA with **2** and **4** under the same conditions.[18] The inset of Figure 3 shows the decrease in ε_{323} values for increasing concentrations of **6**, which reached a plateau upon the addition of 0.75 equiv of complex **6** against TCA, thus providing strong support for the 3:4 self-assembly of **6** and TCA.

Complexation Behaviors of 6, $(Zn_4L^4)^{8+}$, with TCA^{3-} in Aqueous Solution, as Studied by Potentiometric pH Titration. Potentiometric pH titrations of 0.8 mM TCA and a mixture of 0.6 mM **6** and 0.8 mM TCA in an aqueous solution at 25 °C with $I = 0.1$ ($NaNO_3$) were carried out.

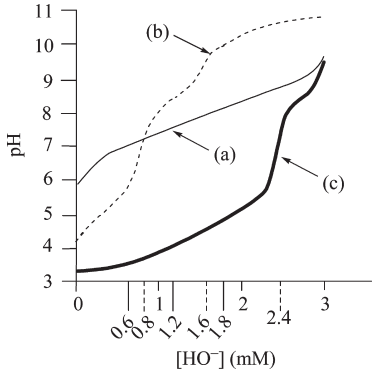

Figure 1. Typical potentiometric pH titration curves for (a) 0.6 mM **6**, $(Zn_4L^4)^{8+}$; (b) 0.8 mM TCA; and (c) 0.6 mM **6** + 0.8 mM TCA, in aqueous solution with $I = 0.1$ ($NaNO_3$) at 25 °C. [HO^-] is the concentration of the base (NaOH) added.

Table 1. Deprotonation Constants for the Zn^{2+}-Bound Waters of Zn^{2+} Complexes (**1**, **2**, **4**, and **6**) Determined by Potentiometric pH Titrations in Aqueous Solution with $I = 0.1$ ($NaNO_3$) at 25 °C

	1, $(ZnL^1)^{2+}$	**2**, $(p\text{-}Zn_2L^2)^{4+}$	**4**, $(p,p\text{-}Zn_3L^3)^{6+}$	**6**, $(Zn_4L^4)^{8+}$
pK_{a1}	7.9 ± 0.1^a	7.9 ± 0.1^b	7.0 ± 0.1^c	6.9 ± 0.1^d
pK_{a2}		7.2 ± 0.1^b	7.4 ± 0.1^c	7.1 ± 0.1^d
pK_{a3}			8.0 ± 0.1^c	8.3 ± 0.1^d
pK_{a4}				8.5 ± 0.1^d

[a] From ref 14a. [b] From ref 14c. [c] From ref 18. [d] Determined in this work.

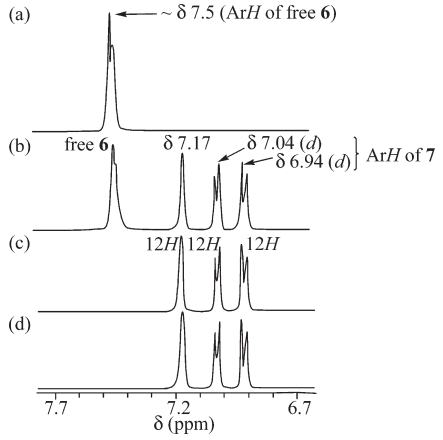

Figure 2. ^1H NMR spectral changes (aromatic region) of **6** after the addition of TCA in D_2O at 25 °C. (a) 3.0 mM **6**, (b) 3.0 mM **6** + 2.0 mM TCA, (c) 3.0 mM **6** + 4.0 mM TCA, and (d) 3.0 mM **6** + 6.0 mM TCA.

The dashed curve b in Figure 1 for TCA gave three pK_a values for TCA: 5.13, 8.24, and 11.7.[17b,18] Curve c in Figure 1 with a distinct break at $[OH^-]_{total} = 2.4$ mM (3 equiv against TCA) supports a scenario in which three protons of TCA (0.8 mM) are deprotonated to bind with all of the Zn^{2+}−cyclen units of **6** under a pH of 6. An analysis of the pH titration curves was in good agreement with the formation of a 3:4 complex of **6** and TCA. The apparent 3:4 complexation constant, K_{app} (defined by eqs 2−4), at pH 7.0 was calculated to be $10^{(41.3\pm2.0)}$ M^{-7}. This value is comparable to the previously reported findings on the 3:3 complex of **4** and TCA, the apparent 3:3 complexation constant for which was $10^{(30.6\pm2.0)}$ M^{-5}.[18] Figure 4a displays a speciation diagram of six possible species, $Zn_4L^4(H_2O)_4^{8+}$, $Zn_4L^4(OH^-)_4^{4+}$, TCA^-, TCA^{2-}, TCA^{3-}, and $\{(Zn_4L^4)_3-(TCA^{3-})_4\}^{12+}$, for a mixture of 0.6 mM **6** and 0.8 mM TCA as a function of pH at 25 °C with $I = 0.1$ ($NaNO_3$). The almost complete formation of a 3:4 complex of **6** and TCA^{3-} is apparent at $6 < pH < 9.8$ and $[Zn_4L^4]_{total} = 0.6$ mM and $[TCA]_{total} = 0.8$ mM. In Figure 4b, the distribution of **7** is compared with that of **5** at $[Zn_4L^4]_{total} = [Zn_3L^3]_{total} = 0.6\ \mu M$, showing that **7** is much more stable than **5** at neutral pH.

Scheme 5. Schematic Presentation of **5** (from X-Ray Crystal Structure Analysis) and Proposed Structure of **7**

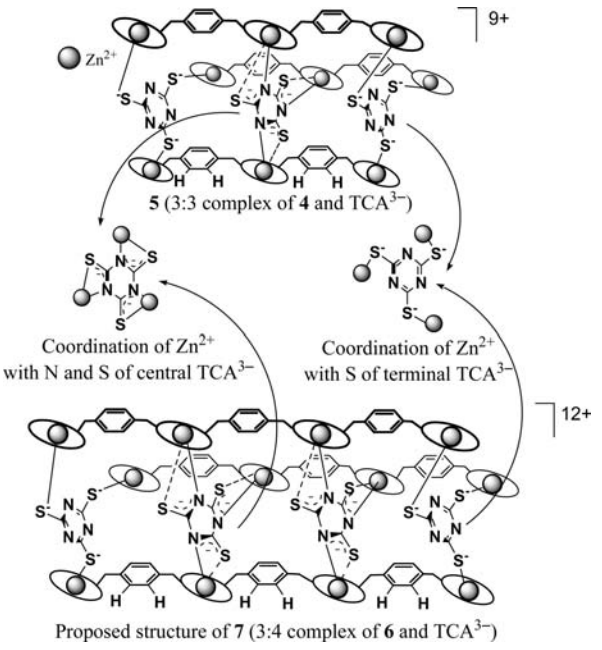

$$3(Zn_4L^4)_{total} + 4(TCA)_{total} \rightleftarrows (Zn_4L^4)_3-(TCA^{3-})_4$$

$$K_{app} = [(Zn_4L^4)_3-(TCA^{3-})_4]/[(Zn_4L^4)_{total}]^3\cdot[(TCA^{3-})]^4(M^{7-}) \quad (2)$$

$$[(Zn_4L^4)_{total}] = [Zn_4L^4\cdot(H_2O)_4] + [Zn_4L^4\cdot(H_2O)_3\cdot(HO^-)] + [Zn_4L^4\cdot(H_2O)_2\cdot(HO^-)_2] + [Zn_4L^4\cdot(H_2O)\cdot(HO^-)_3] + [Zn_4L^4\cdot(HO^-)_4] \quad (3)$$

$$[(TCA)_{total}] = [TCA] + [TCA^-] + [TCA^{2-}] + [TCA^{3-}] \quad (4)$$

ESI MS of Supramolecular Trigonal Prism 7. Figure 5a displays the electrospray ionization time of flight (ESI-TOF) mass spectrum for **7** in H_2O (pH 7.5 ± 0.1), showing m/z peaks for +3, +4, and +6 species of **7**. The observed peaks for the +3 species (Figure 5b) were in good agreement with the theoretical distribution (Figure 5c for +3 species) for the 3:4 complex of **6** and TCA^{3-}.

Effect of Zn^{2+}-Binding Anions Such As Phosphates, Imidates, and Thiolates on the Supramolecular Trigonal Prism 7. The aforementioned ^1H NMR, UV, potentiometric pH titrations, and ESI MS data (Figures 3−5) indicated that **7** is extremely stable in aqueous solution at neutral pH, even at the micromolar level. Figure 6 shows

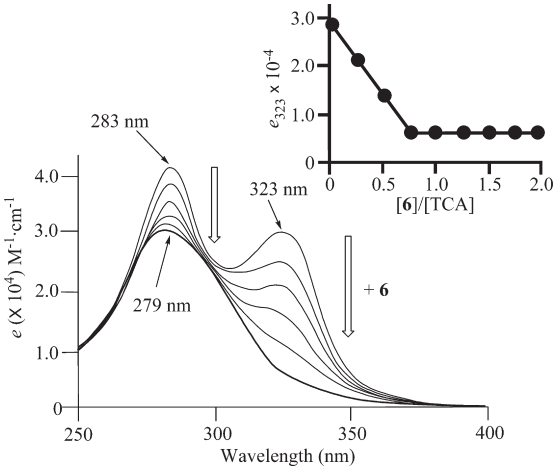

Figure 3. UV spectral change for TCA (30 μM) upon the addition of **6** in 10 mM HEPES (pH 7.4) with I = 0.1 ($NaNO_3$) at 25 °C. The inset shows the decrease in ε_{323} upon changing the ratio of **6** to TCA.

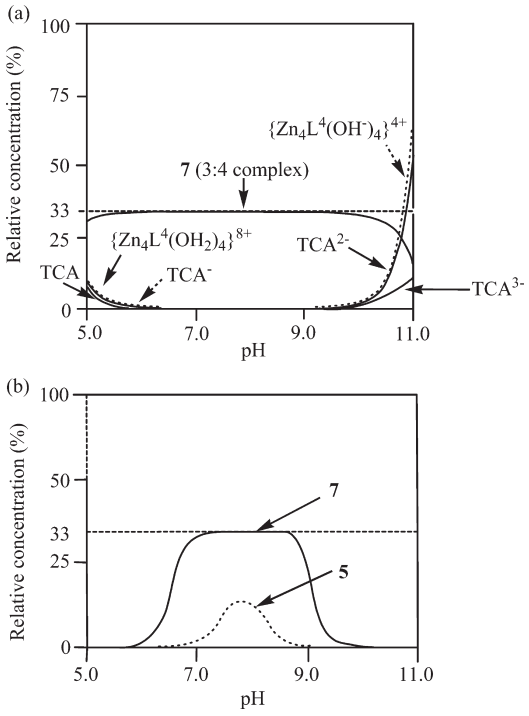

Figure 4. (a) Speciation diagram for **6**, **7**, and TCA species in a mixture of 0.6 mM **6** and 0.8 mM TCA as a function of the pH at 25 °C with I=0.1 ($NaNO_3$). For clarity, species with concentrations less than 5% were omitted. (b) Comparison of pH-dependent concentrations of supramolecular trigonal prisms, **5** (at $[Zn_3L^3]_{total} = [TCA]_{total} = 0.6\ \mu M$) and **7** (at $[Zn_4L^4]_{total} = 0.6\ \mu M$ and $[TCA]_{total} = 0.8\ \mu M$), calculated on the basis of the results of potentiometric pH titrations at 25 °C with I = 0.1 ($NaNO_3$).

changes in UV/vis spectra of **7** and **5** at a pH of 7.4 upon the addition of inorganic phosphate (HPO_4^{2-}) or calf-thymus DNA (ctDNA), which are known to interact with Zn^{2+}−cyclen complexes.[13b,c,g,14e] As shown in Figure 6a, a UV spectrum of **7** (a dashed curve) showed negligible change upon the addition of 100 mM HPO_4^{2-} (a plain curve) and 50 μM (in phosphate) ctDNA (a bold curve). In contrast, the addition of inorganic phosphate (~100 mM) to a solution of **5** induced an increase in the ε value at

(23) The addition of dithiothretol (DTT) and succinimide induced the extensive dissociation of **7** (Figure S1 and S2 in the Supporting Information).

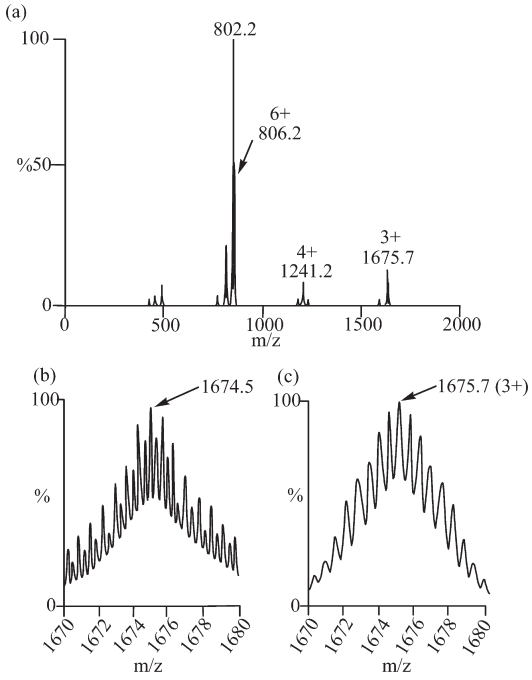

Figure 5. (a) ESI mass spectra of supramolecular trigonal prism **7**. The observed peaks (b) and theoretical distribution (c) for +3 species of **7** ($[7\cdot 9(NO_3)]^{3+}$).

323 nm, corresponding to free TCA^{3-} (Figure 6b), indicating that **5** dissociated to free TCA^{3-} and **4**.[23] Figure 6c clearly displays that **7** is much more stable than **5** in the presence of HPO_4^{2-}.

Interaction on Double-Stranded DNA of Supramolecular Trigonal Prism 7 Determined by an Ethidium Bromide Fluorescence Quenching Assay. Since **7** is a highly cationic (+12) molecule, we expected that **7** would interact with DNA, which is a polyanionic biomacromolecule. It is known that EB (Scheme 6) intercalates into double-stranded DNA (dsDNA), resulting in a considerable enhancement in its fluorescence emission intensity.[24] We thus carried out a competitive assay of **7** and EB with ctDNA. The bold curve and plain curves in Figure 7a are the emission spectra of EB alone (2 μM) and that for a mixture of EB (2 μM) and ctDNA (10 μM in phosphate), respectively, at pH 7.4 and 25 °C, implying that the emission of EB at 590 nm is enhanced by intercalation into DNA (excitation at 510 nm). The addition of **7** (10 μM) to a mixture of EB (2 μM) and ctDNA (10 μM in phosphate) caused a considerable decrease in the emission intensity, as shown by the plain dashed curve. When EB (2 μM) was added to a mixture of ctDNA and **7**, the enhanced emission of EB disappeared completely. Because it was confirmed that **7** dissociates only to a negligible extent in the presence of ctDNA by UV/vis spectra (a bold curve in Figure 6a), we assumed that the trigonal prism **7** interacts with ctDNA as it is (without the dissociation to **6** and TCA) and releases EB from the EB−ctDNA complex.

For comparison, the effect of pentamidine and spermine (Scheme 6) on EB-ctDNA interactions was

(24) (a) LePec, J. B.; Paoletti, C. *J. Mol. Biol.* **1967**, *27*, 87–106. (b) Liu, G. D.; Liao, J. P.; Fang, Y. Z.; Huang, S. S.; Shen, G. L.; Yu, R. Q. *Anal. Sci.* **2002**, *18*, 391–395. (c) Vardevanyan, P. O.; Antonyan, A. P.; Parsadanyan, M. A.; Davtyan, H. G.; Karapetyan, A. T. *Exp. Mol. Med.* **2003**, *35*, 527–533.

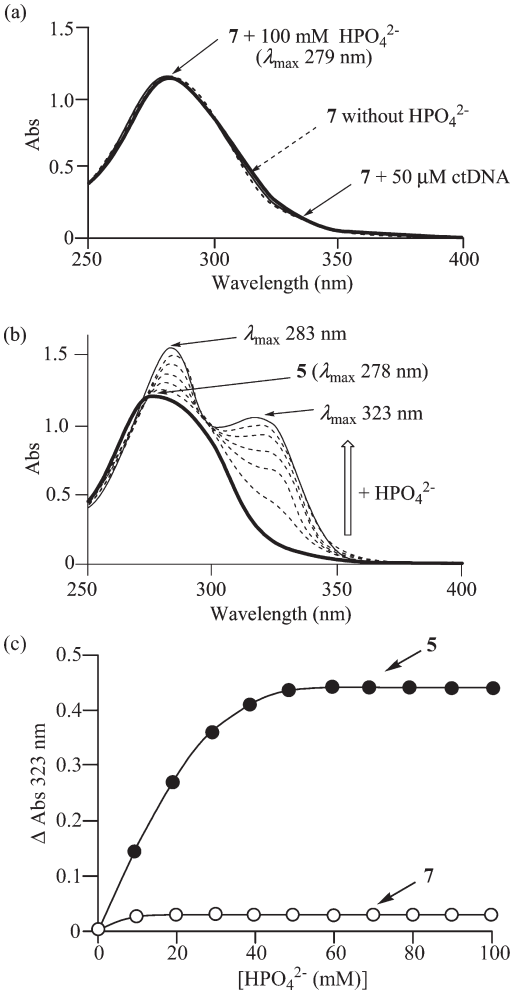

Figure 6. (a) UV spectra of supramolecular trigonal prism **7** (10 μM) in the absence (dashed curve) and presence of 100 mM HPO_4^{2-} (plain curve) and 50 μM (in phosphate) ctDNA (bold curve) in 10 mM HEPES (pH 7.4) with I = 0.1 ($NaNO_3$) at 25 °C. (b) UV spectral change of supramolecular trigonal prism **5** (10 μM) upon the addition of HPO_4^{2-} (0−100 mM) in 10 mM HEPES (pH 7.4) with I = 0.1 ($NaNO_3$) at 25 °C. (c) Change in ε values at 323 nm of **7** (open circle) and **5** (closed circle) upon the addition of HPO_4^{2-} (0−100 mM) in 10 mM HEPES (pH 7.4) with I = 0.1 ($NaNO_3$) at 25 °C ([**5**] = [**7**] = 10 μM).

examined. Pentamidine is a well-known DNA minor groove binder,[25] and spermine interacts with DNA via ionic interactions.[26] As shown in Figure 7a, the addition of 100 μM pentamidine to a solution of the EB−ctDNA complex caused a 42% decrease in emission (bold dashed curve), and the addition of 100 μM spermine caused a 54% decrease (closed circle curve). Figure 7b shows the decrease in fluorescent emission intensity at 590 nm of the EB−ctDNA complex at increasing concentrations of **7**, pentamidine, and spermine. Utilizing eqs 5−7,[24c] where C_T, C_B, and C_F are the total concentrations of added **7**, DNA-bound **7**, and free **7**, respectively, and n is the

Scheme 6

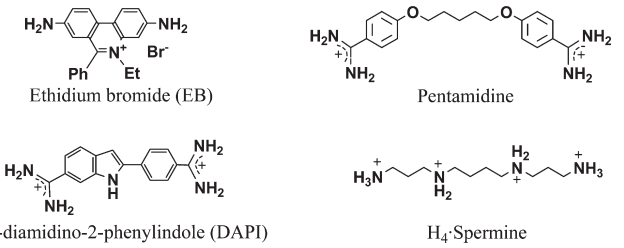

binding-site number per base pair. The complexation constant (K_s) for **7** and ctDNA was calculated to be 4 ± 2 μM, using the reported complexation constant for the EB−ctDNA complex of 12.3 μM.[27]

$$C_B = C_T - C_F \quad (5)$$

$$r = C_B/[\mathrm{DNA} + \mathrm{EB}] \quad (6)$$

$$r/C_F = K_s(1 - nr)/[(1 - nr)/[1 - (n-1)]]^{n-1} \quad (7)$$

Effect of 7 on the Melting Temperature (T_m) of Calf-Thymus DNA. When dsDNA polymers are heated slowly, the double helixes "melt" to give single-stranded species, which can be detected by the "hypochromic effect" in the UV absorption of the nucleobases. The midpoint temperature of this transition is the melting temperature (T_m) of the double-stranded DNA. Thus, we examined the effect of **7**, **6**, and two DNA minor groove binders, DAPI[28] and pentamidine[25] (see Scheme 6), on the T_m values of ctDNA. As shown in Figure 8 and Table 2, the T_m value for ctDNA (50 μM in phosphate) with no additive (r = 0, where r = [additive]/[base in phosphate]) was determined to be 65 ± 0.5 °C. The addition of **7** had a negligible effect on the T_m value of ctDNA at r = 0.01−0.03 (corresponding to [**6**]/[DNA] = 0.03−0.09), as shown in Figure 8a. We have observed negligible change in the UV absorption intensity of **7** (10 μM) at 323 nm in 10 mM HEPES (pH 7.4 at 25 °C) from 25 to 85 °C in the absence and presence of ctDNA (50 μM in phosphate), which indicates that **7** is thermally stable and hardly dissociates into **6** and TCA^{3-} below 85 °C, even in the presence of DNA. On the other hand, the addition of **6** (r = 0.01−0.05) lowered the T_m value, as shown in Figure 8b and Table 2, possibly due to the disruption of hydrogen bonding between complementary base pairs in DNA by Zn^{2+}−thymidine complexation.[14] As shown in Figure 9a and 9c, the addition of DAPI (r' = 0.01 and 0.03) and pentamidine (r' = 0.1) resulted in an increase in the T_m value of ctDNA, due to the stabilization of the double strands of ctDNA.[11l,14d,k] Very interestingly, the T_m curve of ctDNA (50 μM in phosphate) in the presence of DAPI (r' = 0.03) and **7** (r = 0.03) and that in the presence of pentamidine (r' = 0.1) and **7** (r = 0.05) were nearly identical to that of ctDNA alone (Figure 9b,c and Table 2). These facts suggest that the stabilizing effect of the ctDNA by DAPI and pentamidine is neutralized by **7**.

Gel Mobility Shift Assay of Double-Stranded DNA with Supramolecular Trigonal Prism 7. The results of an EB

(25) Edwards, K. J.; Jenkins, T. C.; Neidle, S. *Biochemistry* **1992**, *31*, 7104–7109.
(26) (a) Morgan, A. R.; Lee, J. S.; Pulleyblank, D. E.; Murray, N. L.; Evans, D. H. *Nucleic Acids Res.* **1979**, *7*, 547–569. (b) Antony, T.; Thomas, T.; Shirahata, A.; Thomas, T. J. *Biochemistry* **1999**, *38*, 10775–10784. (c) Blagbrough, I. S.; Adjimatera, N., Ahmed, O. A. A.; Neal, A. P.; Pourzand, C. *Neurotox '03: Neurotoxicological Targets from Functional Genomics and Proteomics*; Beadle, D. J., Mellor, I. R., Usherwood, P. N. R., Eds.; Society of Chemical Industry: New York, 2004; Chapter 16.
(27) Garbet, N. H.; Hammond, N. B.; Graves, D. E. *Biophys. J.* **2004**, *87*, 3974–3981.
(28) Špačková, N.; Cheatham, T. E.; Ryjáček, F.; Lankaš, F.; van Meervelt, L.; Hobza, P.; Šponer, J. *J. Am. Chem. Soc.* **2003**, *125*, 1759–1769.

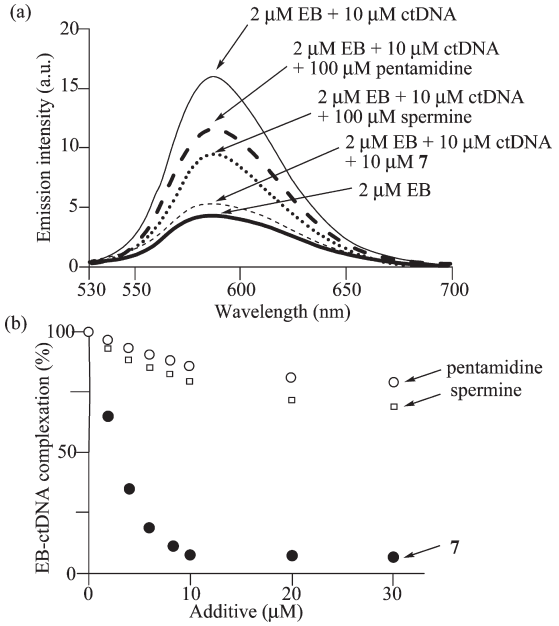

Figure 7. (a) Change in fluorescence emission of the EB−ctDNA complex upon the addition of supramolecular trigonal prism **7** or other DNA binders in 10 mM HEPES (pH 7.4) with $I = 0.1$ ($NaNO_3$) at 25 °C (excitation at 510 nm). Bold curve, 2 μM EB alone; plain curve, 2 μM EB + 10 μM ctDNA; plain dashed curve, 2 μM EB + 10 μM ctDNA + 10 μM **7**; bold dashed curve, 2 μM EB + 10 μM ctDNA + 100 μM pentamidine; and close circle curve, 2 μM EB + 10 μM ctDNA + 100 μM spermine in 10 mM HEPES (pH 7.4) with $I = 0.1$ ($NaNO_3$) at 25 °C. The term a.u. represents an arbitrary unit. (b) Decrease in the EB−ctDNA complex in a reaction mixture of 2 μM EB and 10 μM (in phosphate) ctDNA upon the addition of **7** (closed circle), pentamidine (open circle), and spermine (open square) in 10 mM HEPES (pH 7.4) with $I = 0.1$ ($NaNO_3$) at 25 °C (excitation at 510 nm).

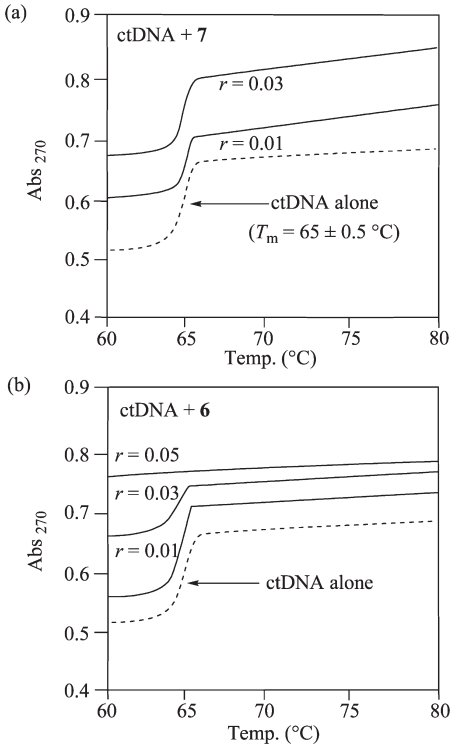

Figure 8. Change in thermal melting (T_m) curves of 50 μM (in phosphate) ctDNA upon the addition of (a) **7** and (b) **6** at pH 7.4 (10 mM HEPES) with $I = 0.02$ ($NaNO_3$) (r = [**7** or **6**]/[ctDNA in phosphate]).

Table 2. T_m Values of ctDNA upon the Addition of **7**, **6**, DAPI, and Pentamidine (r = [**7** or **6**]/[ctDNA in phosphate], r' = [DAPI or pentamidine]/[ctDNA in phosphate])

additive	r	r'	T_m (°C)	ΔT_m (°C)
none			65	
7	0.01		65	0
	0.02		65	0
	0.03		65	0
6	0.01		65	0
	0.02		65	0
	0.03		64	−1
	0.04		63	−2
	0.05		disappeared	
DAPI		0.01	70	+5
		0.03	77	+12
7 + DAPI	0.01	0.03	65	0
	0.02	0.03	65	0
	0.03	0.03	65	0
pentamidine		0.1	72	+7
7 + pentamidine	0.05	0.1	65	0

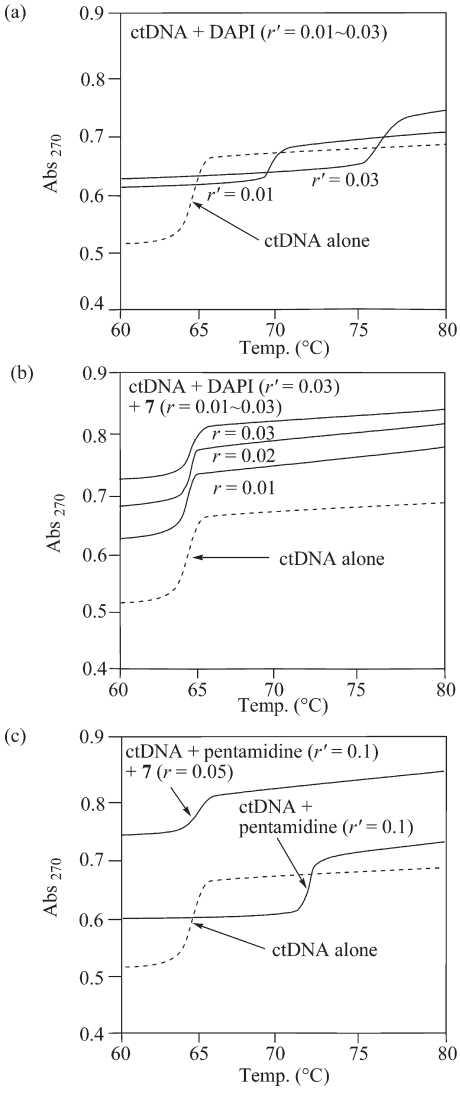

Figure 9. Change in thermal melting (T_m) curve of 50 μM (in phosphate) ctDNA upon the addition of (a) DAPI, (b) DAPI + **7**, and (c) pentamidine and pentamidine + **7**, at pH 7.4 (10 mM HEPES) with $I = 0.02$ ($NaNO_3$) (r = [additive]/[ctDNA in phosphate]). In b and c, r' values for DAPI and pentamidine were 0.03 and 0.1, respectively.

displacement experiment of ctDNA with the trigonal prism **7** (Figure 7) suggested that **7** interacts strongly with ctDNA. On the other hand, T_m measurements of ctDNA in the presence of **7** (Figure 8 and 9) indicated that **7** interacts negligibly with ctDNA. In order to further examine this paradox, we conducted a GMSA of DNA with **7**. The double-stranded DNA fragment (150 bp) used in this experiment was obtained by the polymerase chain reaction (PCR) of plasmid pUC18 using 5′ labeled with fluorescent dye 6-fluorescein (FAM) primers. Reaction mixtures of DNA and **7** at various concentrations (0−3.0 μM) were applied to polyacrylamide gel electrophoresis (PAGE) and separated at room temperature at 10 V/cm. As shown in Figure 10, the fluorescence intensity of the DNA bands decreases with increasing concentrations of **7**. Analysis of these results gave the concentration for the 50% complexation (IC_{50}) of **7** with DNA of 2 ± 1 μM, which coincided reasonably well with the K_d value of 4 ± 2 μM determined by the EB displacement assay using ctDNA (Figure 7).

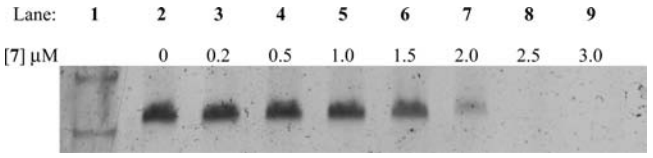

Figure 10. The results of PAGE (7.5%) of 5′FAM pUC18 (15 μg/50 μL) incubated with various concentrations of **7** for 30 min at 25 °C and pH 7.4 (10 mM HEPES): lane 1, DNA ladder; lane 2, [**7**] = 0 μM; lane 3, [**7**] = 0.2 μM; lane 4, [**7**] = 0.5 μM; lane 5, [**7**] = 1.0 μM; lane 6, [**7**] = 1.5 μM; lane 7, [**7**] = 2.0 μM; lane 8, [**7**] = 2.5 μM; lane 9, [**7**] = 3.0 μM.

Our speculation on the interaction of **7** with ctDNA, based on the above experimental results, is summarized in Scheme 7. We assume that the ionic interaction between **7** and dsDNA is important for achieving complexation, as shown in **14**, which disturbs the interaction of DNA with EB, DAPI, and pentamidine. It is interesting to note that **7** induces the dissociation of EB−DNA (**15a**), DAPI−DNA (**15b**), and spermine−DNA (**15c**) complexes, as evidenced by an EB fluorescence quenching assay and

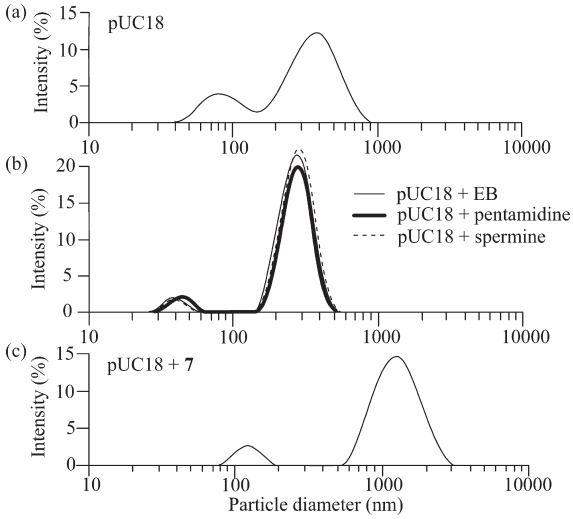

Figure 11. Particle diameter distribution in the intensity of (a) pUC18 alone (15 μg/200 μL), (b) pUC18 + EB/pentamidine/spermine, and (c) pUC18 + **7** at pH 7.4 (10 mM HEPES) and $I = 0.02$ ($NaNO_3$).

Scheme 7

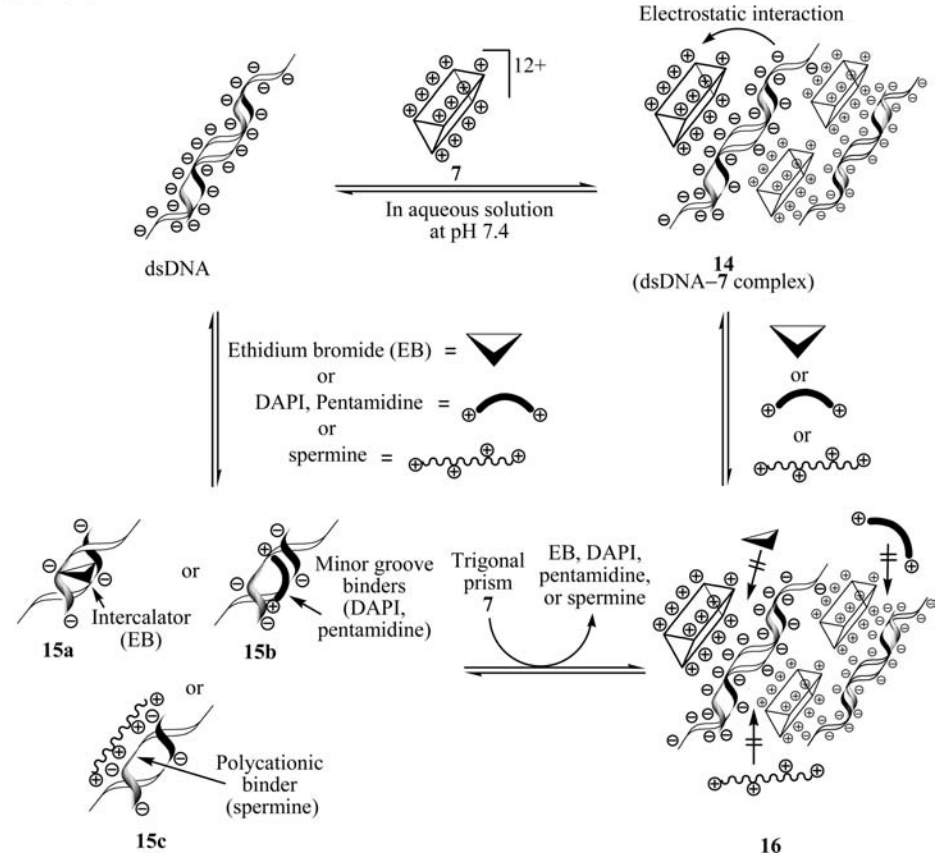

thermal melting experiments of ctDNA, while **7** itself has only a negligible effect on the T_m of ctDNA. Therefore, we hypothesize that **7** and dsDNA aggregate mainly due to electrostatic interactions[29] to inhibit the complexation of DNA with a DNA intercalator (EB), minor groove binders (DAPI and pentamidine), and a polycationic DNA binder (spermine), as illustrated in **16** in Scheme 7, albeit **7** does not affect the thermodynamic stability of DNA.

Dynamic Light-Scattering Measurements on Supramolecular Trigonal Prism 7−5′FAM pUC18 Complex. The complexation of **7** with 5′FAM pUC18 was further examined by means of a DLS method, which is based on fluctuations in the intensity of light as the result of the diffusion of nanoparticles by Brownian motion.[30,31] Figure 11a shows the distribution in the intensity of particles with a diameter (ca. 320 nm on average) of 15 μg/200 μL of pUC18 alone. In the presence of EB or pentamidine or spermine (at 4 μM), the particle size of pUC18 became somehow smaller than that of pUC18 itself (Figure 11b). In striking contrast, the addition of **7** (4 μM) to pUC18 induced an increase in particle diameter to ca. 980 nm on average (Figure 11c).[32] Considering the collective experimental results presented herein, we conclude that the supramolecular trigonal prism **7** functions as a polycationic template for the aggregation of polyanionic DNA but does not change the thermal stability of double-stranded DNA, as summarized in Scheme 7.[33]

Conclusions

In this work, we report on the successful formation of a supramolecular trigonal prism, **7**, $\{(Zn_4L^4)_3-(TCA^{3-})_4\}^{12+}$, by the self-assembly of linear tetrakis(Zn^{2+}−cyclen) complex **6**, $(Zn_4L^4)^{8+}$, with TCA^{3-}. The complex is quite stable at submicromolar concentrations in aqueous solution, as evidenced by ^{1}H NMR, potentiometric pH titration, UV/vis spectrophotometric titrations, and MS spectra. The findings also show that **7** interacts with double-stranded DNA, as confirmed by EB displacement assays and GMSA. Although **7** induced only negligible change in the T_m values of dsDNA, it inhibited the interaction of DNA and DNA binders such as EB, DAPI, pentamidine, and spermine. The DLS results indicate that **7** functions as a polycationic template to induce aggregation of dsDNA, possibly due to the electrostatic interactions. The result should be useful in further attempts to design stable supramolecular complexes and their applications in areas of the molecular recognition of biological molecules and drug design.

Experimental Section

General Information. All reagents and solvents were purchased commercially, were of the highest quality, and were used without further purification. All aqueous solutions were prepared using deionized, distilled water. The Good's buffers (Dojindo) were obtained from commercial sources: HEPES (2-(4-(2-hydroxyethyl)-1-piperazinyl) ethanesulfonic acid, pK_a = 7.6). Stock aqueous solutions of 10 mM pentamidine (Sigma), 10 mM DAPI (Sigma), 10 mM spermine (Nacalai Tesque, Inc.), and 3 mM ethidium bromide (Sigma) were prepared using deionized, distilled water and stored at −20 °C. Concentrations were determined from visible absorbance maxima using previously determined molar extinction coefficients, DAPI (ε_{342} = 23 000 M^{-1} cm^{-1}),[34] and ethidium bromide (ε_{478} = 5680 M^{-1} cm^{-1})[35] in aqueous solution. Calf thymus DNA (Sigma) was dissolved in water, sonicated, and filtered before use, and its concentration was determined spectrophotometrically (ε_{260} = 6600 M^{-1} cm^{-1}).[36] Ex Taq, 10× Ex Taq buffer, dNTP mixture (all from Takara-bio Co.), and pUC 18 (Toyobo Co., Ltd.) were stored at −20 °C prior to use. UV spectra and fluorescence spectra were recorded on a JASCO V-550 spectrophotometer and a FP-6500 spectrofluorometer, equipped with a temperature controller unit at 25 ± 0.1 °C, respectively. IR spectra were recorded on a Horiba FTIR-710 spectrophotometer at room temperature. Melting points were measured by a Yanaco MP-J3 micromelting point apparatus and are uncorrected. ^{1}H (500 MHz) and ^{13}C (125 MHz) NMR spectra at 25 ± 0.1 °C were recorded on a JEOL Delta 500 spectrometer. 3-(Trimethylsilyl) propionic-2,2,3,3-d_4 acid sodium salt in D_2O and tetramethylsilane in $CDCl_3$ were used as external and internal references, respectively, for ^{1}H and ^{13}C NMR measurements. The pD values in D_2O were corrected for a deuterium isotope effect using pD = [pH-meter reading] + 0.40. The ESI-TOF mass spectra were recorded on a JEOL JMS-P100CS (cold spray positive). Circular dichroism (CD) spectra were recorded (given in the Supporting Information) on an Applied Photophysics Chirascan CD Spectrometer. Elemental analyses were performed on a Perkin-Elmer CHN 2400 series II CHNS/O analyzer at the Natural Science Center for Basic Research and Development (N-BARD), Hiroshima University. Thin-layer chromatography (TLC) and silica gel column chromatography were performed using Merck Art. 5554 (silica gel) TLC plates and Fuji Silysia Chemical FL-100D (silica gel), respectively.

[1,4-Bis(4,7,10-tris(*tert*-butyloxycarbonyl)-1,4,7,10-tetraazacyclododecane-1-ylmethyl)(1,7-bis(diethoxyphosphoryl)- 1,4,7,10-tetraazacyclododecane-1-ylmethyl)benzene, 11. A mixture of 1-bromomethyl-4-(4,7,10-tris(*tert*-butyloxycarbonyl)-1,4,7,10-tetraazacyclododecan-1-ylmethyl)benzene,[20] **9** (1.0 g, 1.52 mmol); 1,7-bis(diethoxyphosphoryl)-1,4,7,10-tetraazacyclododecane, **10** (1.36 g, 2.67 mmol); and Cs_2CO_3 (1.0 g, 3.07 mmol) in CH_3CN was stirred at reflux for two days. After removing insoluble inorganic salts by filtration, the filtrate was concentrated under reduced pressure and the resulting residue purified by silica gel column chromatography (AcOEt/MeOH = 9:1) to give **11** as a yellow colored amorphous solid (0.8 g, 51% yield). IR (KBr pellet): 3472, 2978, 2932, 1685, 1458, 1416, 1252, 1171, 1024, 964, 772 cm^{-1}. ^{1}H NMR (500 MHz, $CDCl_3$/TMS): δ 1.35 (12H, t, J = 7.1, CH_3), 1.48 (27H, brs, $C(CH_3)_3$), 2.65−2.84 (8H, m, NCH_2), 3.25−3.71 (36H, m, NCH_2, $ArCH_2$, CH_2), 7.13 (2H, d, J = 8.0, ArH), 7.21 (2H, d, J = 8.0, ArH). ^{13}C NMR (125 MHz, $CDCl_3$/TMS): δ 16.24, 16.29, 28.51, 28.74, 44.38, 45.29, 45.80, 48.05, 48.43, 49.23, 49.49, 62.80, 62.84, 63.08, 63.17, 79.46, 79.54, 130.45, 155.77, 155.80.

1,4-Bis(1,4-bis(4,7,10-tris(*tert*-butyloxycarbonyl)-1,4,7,10-tetraazacyclododecan-1-ylmethyl)-(1,7-bis(diethoxyphosphoryl)-1,4,7,10-tetraazacyclododecane-1-ylmethyl)benzyl)benzene, 12. A mixture of

(29) Shiraishi, T.; Hamzavi, R.; Nielsen, P. E. *Nucleic Acids Res.* **2008**, *36*, 4424–4432.
(30) Finsy, R. *Colloid Interface Sci.* **1994**, *52*, 79–143.
(31) Vijayanathan, V.; Thomas, T.; Shirahata, A.; Thomas, T. J. *Biochemistry* **2001**, *40*, 13644–13651.
(32) Similar behaviors were observed for ctDNA upon the addition of EB, pentamidine, spermine, and **7** (Figure S3 in the Supporting Information).
(33) Our preliminary experiments have indicated that **7** induces considerable red shifts in circular dichroism (CD) spectra of ctDNA, while pentamidine and spermine induced small changes in CD spectra of ctDNA (Figure S4 in the Supporting Information). The detail has been examined.
(34) Trotta, E.; D'Ambrosio, E.; Del Grosso, N.; Ravagnan, G.; Cirilli, M.; Paci, M. *J. Biol. Chem.* **1993**, *268*, 3944–3951.
(35) Firth, W. J.; Watkins, C. L.; Graves, D. E.; Yielding, L. W. *J. Heterocycl. Chem.* **1983**, *20*, 759–765.
(36) Wells, R. D.; Larson, J. E.; Grant, R. C.; Shortle, B. E.; Cantor, C. R. *J. Mol. Biol.* **1970**, *54*, 465–497.

11 (700 mg, 0.65 mmol), *p*-bis(bromomethylbenzene) (90 mg, 0.34 mmol), and Cs_2CO_3 (442 mg, 1.35 mmol) in CH_3CN (10 mL) was stirred at reflux for two days. After the insoluble inorganic salts were removed by filtration, the filtrate was concentrated under reduced pressure and the residue purified by silica gel column chromatography (CH_2Cl_2/MeOH = 1:0−40:1−20:1−3:1−0:1) to give **12** as a yellow colored amorphous solid (235 mg, 32% yield). IR (KBr pellet): 3437, 2965, 1615, 1454, 1417, 1219, 862, 763 cm^{-1}. ^1H NMR (500 MHz, $CDCl_3$/TMS): δ 1.18 (24H, t, J = 7.1, CH_3), 1.43 (54H, brs, $C(CH_3)_3$), 2.65−2.84 (24H, m, NCH_2), 3.25−3.71 (68H, m, NCH_2, $ArCH_2$, CH_2), 7.16 (6H, d, J = 7.8, ArH), 7.24 (6H, d, J = 7.8, ArH). ^{13}C NMR (125 MHz, $CDCl_3$/TMS): δ 16.18, 16.24, 28.51, 28.74, 44.20, 47.33, 47.63, 47.07, 49.92, 49.99, 53.76, 59.84, 61.27, 61.85, 61.89, 79.34, 79.45, 129.28, 130.30, 155.36, 156.12.

1,4-Bis(1,4-bis(1,4,7,10-tetraazacyclododecan-1-ylmethyl)benzyl)-benzene Dodecahydrobromide Octahydrate·12HBr·8H_2O, 13. An aqueous 47% HBr (4 mL) solution was added dropwise to a solution of **12** (100 mg, 0.04 mmol) in EtOH (10 mL) at 0 °C. After stirring overnight at room temperature, the reaction mixture was concentrated under reduced pressure. The resulting crude powder was crystallized from 47% aqueous HBr/EtOH to give **13** as a colorless powder (69.3 mg, 91% yield). IR (KBr pellet): 3451, 3243, 2921, 2340, 1383, 1090, 825, 1024 cm^{-1}. ^1H NMR (500 MHz, D_2O/external TSP): δ 2.98−3.33 (64H, m, NCH), 3.96−3.98 (12H, m, ArCHN), 7.48−7.49 (12H, m, ArH). ^{13}C NMR (125 MHz, D_2O/external TSP): δ 42.42, 42.63, 43.19, 44.90, 47.64, 48.44, 56.39, 56.58, 130.83, 130.96, 131.02, 135.05, 135.10. Elem Anal. Calcd for $C_{56}H_{126}N_{16}O_8Br_{12}$: C, 31.87; H, 6.02; N, 10.62. Found: C, 32.09; H, 6.02; N, 10.17.

1,4-Bis(1,4-bis(1,4,7,10-tetraazacyclododecan-1-ylmethyl)benzyl)-benzene Tetra(zinc(II)), Complex 6·(8NO_3^-·5.5H_2O). The pH of a solution of **13**·12HBr·8H_2O (55 mg, 0.26 mmol) was adjusted to 12 with a 5 N NaOH aqueous solution. The alkaline solution was extracted with $CHCl_3$ (50 mL×3), and the combined organic layers were dried over anhydrous Na_2SO_4, filtered, and concentrated under reduced pressure. The resulting residue was dissolved in EtOH (5 mL), to which a solution of $Zn(NO_3)_2$·$(H_2O)_6$ (32 mg, 1.1 mmol) in EtOH/H_2O was added. After stirring at 60 °C overnight, the reaction mixture was concentrated under reduced pressure, and the resulting residue was crystallized from H_2O/EtOH to give **6** as a colorless powder (44.3 mg, 92% yield). Mp > 250 °C. IR (KBr pellet): 3471, 1612, 1512, 1246, 1124, 619 cm^{-1}. ^1H NMR (500 MHz, D_2O/external TSP): δ 2.72−3.25 (64H, m, NCH_2), 4.05 (12H, s, $ArCH_2N$), 7.46−7.47 (12H, m, ArH). ^{13}C NMR (125 MHz, D_2O/external TSP): δ 31.2, 44.8, 46.3, 47.1, 51.6, 57.7, 67.7, 117.4, 127.2, 135.2, 161.0. Elem Anal. Calcd for $C_{56}H_{109}N_{24}O_{29.5}Zn_4$: C, 36.28; H, 5.99; N, 18.14. Found: C, 36.74; H, 6.03; N, 17.72.

Isolation of 7·(12NO_3^-·35H_2O). Complex **6**·8(NO_3^-)·5.5H_2O (52 mg, 0.03 mmol), TCA (6.6 mg, 0.04 mmol), and $NaNO_3$ (49 mg, 0.56 mmol) were dissolved in H_2O (3 mL) and the pH adjusted to 8.0 ± 0.1 by the addition of aqueous NaOH. The entire mixture was filtered and allowed to slowly evaporate in vacuo for one week, to give **7**·$(NO_3^-)_{12}$·35H_2O (11 mg, 20% yield). Mp > 250 °C. IR (KBr pellet): 3471, 1612, 1512, 1246, 1124, 619 cm^{-1}. ^1H NMR (500 MHz, D_2O/external TSP): δ 2.60−2.92 (120H, m, CH_2 of cyclen), 3.02−3.18 (26H, m, CH_2 of cyclen), 3.26−3.52 (46H, m, CH_2 of cyclen), 3.86 (36H, brs, $ArCH_2$), 6.88−6.94 (12H, m, ArH), 7.00−7.06 (12H, m, ArH), 7.12−7.18 (12H, m, ArH). ^{13}C NMR (125 MHz, D_2O/DMSO-d_6): δ 44.4, 46.4, 48.9, 49.2, 56.5, 132.2, 132.5, 133.8. Elem Anal. Calcd for $C_{180}H_{364}N_{72}O_{71}S_{12}Zn_{12}$: C, 37.00; H, 6.28; N, 17.26. Found: C, 36.51; H, 5.74; N, 17.09.

UV Spectrophotometric Titration and Fluorescence Titration. UV spectra and fluorescence emission spectra were recorded on a JASCO V-550 UV/vis spectrophotometer and a JASCO FP-6500 spectrofluorometer, respectively, at 25.0 ± 0.1 °C. For fluorescence titrations, a sample solution in a 1 cm quartz cuvette was excited at the isosbestic points determined by UV titrations. The resulting UV titration data (changes in ε values at a given wavelength) were analyzed for apparent complexation constants, K_{app}, using the Bind Works program (Calorimetry Sciences Corp).

Potentiometric pH Titrations. The electrode system (Orion Research Expandable Ion Analyzer EA920 with a Ross Combination pH Electrode 8102 BN) was calibrated daily as follows: An aqueous solution (50 mL) containing 4.0 mM of HCl and 96.0 mM of $NaNO_3$ (i.e., I = 0.1) was prepared under an argon (> 99.999% purity) atmosphere at 25.0 ± 0.1 °C, and the first pH value (pH_1) was read. The theoretical pH values corresponding to pH_1 and pH_2 were calculated: pH_1' = 2.481 and pH_2' = 11.447, using K_W (= $a_{H^+} \times a_{OH^-}$) = $10^{-14.00}$, K'_W (= $[H^+][OH^-]$) = $10^{-13.79}$, and f_{H^+} = 0.825. The corrected pH values ($-\log a_{H^+}$) were obtained using the following equations: $a = (pH_2' - pH_1')/(pH_2 - pH_1)$; $b = pH_2' - a \times pH_2$; $pH = a \times$ (pH-meter reading) + b.

The potentiometric pH titrations were carried out with I = 0.1 ($NaNO_3$) at 25.0 ± 0.1 °C, where at least two independent titrations were always performed. Deprotonation constants and complexation constants K (defined in the text) were determined by means of the BEST program.[22] The pH σ fit values defined in the program are less than 0.02. The obtained constants containing a term of $[H^+]$ were converted to the corresponding mixed constants using $[H^+] = a_{H^+}/f_{H^+}$. The species distribution values (%) against pH (= $-\log a_{H^+}$) were obtained using the SPE program.[22]

Thermal Denaturation Studies. Thermal denaturation processes of calf-thymus DNA (50 μM in phosphate) in a 10 mM HEPES buffer (pH 7.4 at 25 °C) containing 20 mM $NaNO_3$ were followed on a JASCO V-550 UV/vis spectrophotometer equipped with a thermoelectric cell temperature controller (±0.5 °C) and a stirring unit. A 1 cm quartz cuvette was used. T_m values were determined graphically for each sample from the spectral data. The ΔT_m value for each compound was determined as the temperature difference between the compound T_m and the DNA T_m. Thermal melting curves for calf thymus with and without the sample were obtained by following the absorption change at 260 or 270 nm as a function of the temperature.

Electrospray Ionization MS of Supramolecular Trigonal Prism 7. ESI mass spectra were recorded on a JEOL JMS-P100CS (cold spray positive). Aqueous solutions (100−200 ng/μL) of given complexes were analyzed by direct infusion at 10 μL/min. Mass spectra were scanned in the m/z range of 100−2000 at 1 s/scan with an interscan delay of 0.1 s. Data were processed by using the spectrometer software "Mass Center". Theoretical distribution for the +3 to +6 species for **7** with mass-to-charge ratios (m/z) were calculated by using the program "Mass Center".

Preparation of 5′FAM-Labeled pUC18 DNA Fragments. The 150 bp DNA fragment (pUC18 sequence from 1341 to 1490) was amplified by PCR using pUC18 as a template and two 19-mer primers (5′-AGTTACCTTCGGAAAAAGA-3′ and 5′-GCGTCAGACCCCGTAGAAA-3′) obtained from Gene Design, Inc. and Texas Genomic Japan. The 5′ end of the 5′-AGTTACCTTCGGAAAAAGA-3′ primer was labeled with FAM. The amplified DNA fragments were purified by agarose gel electrophoresis and extracted using phenol/chloroform and finally precipitated with ethanol. The amount of extracted DNA was determined by UV absorption at 260 nm.

Gel Mobility Shift Assay Studies. A mixture of DNA (15 μg of 5′FAM-labeled pUC18 DNA) with a various concentrations of **7** in 50 μL of 10 mM HEPES (pH 7.4) was incubated at 25 °C for 30 min, to which 3 μL of loading buffer was added. From these solutions, 44 μL aliquots were loaded on a 7.5% polyacrylamide gel. Electrophoresis was carried out in 7.5% polyacrylamide gels under native conditions at a constant voltage (100 V, 10 V/cm). The running buffer was 0.5× TBE (89 mM Tris-borate, pH 8.0,

1.0 mM EDTA). After completion of the electrophoresis, the gels were analyzed using an FLA-2000 (FUJIFILM) apparatus scanned by an argon laser at 488 nm, and the fluorescence of the free and complexed DNA was measured in the wavelength intervals 515−545 nm (530DF30-filter, analysis of FAM fluorescence).

Dynamic Light-Scattering Studies. Measurement of the size in diameter of the **7** + 5′FAM pUC18 and **7** + ctDNA complexation and other compounds were made with DLS at 25 °C using a Zetasizer Nano ZS (Malvern Instruments) spectrometer, the detection range of which is 0.6−10 000 nm. The instrument was equipped with a 4 mW He−Ne laser operating at 623 nm, and samples were placed in a 40 μL micro-volume plastic cuvette. All samples were prepared and incubated in 10 mM HEPES (pH 7.4) with the ionic strength adjusted by $NaNO_3$ (I = 0.02) and containing either 15 μg/200 μL of 5′FAM pUC18 or 100 μM of ctDNA in phosphate concentration.

Acknowledgment. This work was supported by the Grants-in-Aid from the Ministry of Education, Science and Culture in Japan (No. 15990008, 18390009, and 19659026). S.A. and M.Z. are thankful for the grant and the postdoctoral fellowship for foreign researchers from Japan Society for the Promotion of Science (JSPS), No. 20-08451. We thank to Ms. Mai Kobayashi from JEOL Ltd. (Japan) for the ESI-TOF mass spectra. We are thankful to Dr. Kazuhiro Nakashima and Mr. Shunsuke Nomura from the Sysmex Corporation (Japan) for the DLS measurements and to Dr. Matthew Pope from Applied Photophysics, Ltd. (UK) and Mr. Shuichi Yoshida from Tega Science (Japan) for the CD measurements.

Supporting Information Available: Figures S1−S4 showing the UV spectral changes of **7** and **5** upon the addition of succinimide and dithiothreitol, DLS measurements, and CD measurements. This material is available free of charge via the Internet at http://pubs.acs.org.